

The Group Evolution Multiwavelength Study (GEMS): The near-infrared luminosity function of nearby galaxy groups

Trevor A. Miles*, Somak Raychaudhury & Paul A. Russell

School of Physics and Astronomy, University of Birmingham, Edgbaston, Birmingham B15 2TT, UK

MNRAS submitted - 2006 January; accepted - 2006 September

ABSTRACT

We present J and K -band luminosity functions (LF) for the Group Evolution Multiwavelength Study (GEMS) sample of 60 nearby groups of galaxies, with photometry from the 2MASS survey. We find that, as seen in B and R -band photometry of a subsample of these groups in our earlier work, the LFs of the X-ray dim groups ($L_X < 10^{41.7}$ erg s $^{-1}$) show a depletion of galaxies of intermediate luminosity around $M_K = -23$, within a radius $0.3 R_{500}$ from the centres of these groups. This feature is not seen in the X-ray brighter groups, nor in either kind of group when the LFs are determined all the way out to R_{500} . We conclude that an enhanced level of star formation is not responsible for this feature. From the faint end of the LFs, we find support for the under-abundance of low surface brightness dwarfs in the 2MASS survey. We find that for all kinds of groups, the modelling of the luminosity function, with universal forms for the LFs of galaxies of different morphological types, fails when simultaneously required to fit the B and K -band LFs. This means that the dip-like features seen in LFs are not merely due to the varying proportions of galaxies of different morphological types among the X-ray dim and bright groups. We argue that this supports our hypothesis that this feature is due to the enhanced merging of intermediate-mass galaxies in the dynamically sluggish environment of X-ray dim groups.

Key words: galaxies: luminosity functions — galaxies: evolution — galaxies: structure — galaxies: clusters

1 INTRODUCTION

Luminosity functions of galaxies are an essential ingredient in the study of galaxy formation. Numerical models involving merging, cooling and feedback (*e.g.*, Somerville & Primack 1999; Kauffmann et al. 1999; Benson et al. 2003) produce definite predictions for the luminosity function in various environments, which can now be compared with photometric observations of wide-field and deep samples of galaxies of the field and in highly clustered regions.

The galaxian luminosity function (LF) is usually modelled as the Schechter function, which drops sharply at bright magnitudes, but rises at the faint end as a power-law of slope α . In cold dark matter (CDM) dominated models; dwarf galaxy haloes collapsing at $z > 3$ have very efficient cooling, resulting in a steep slope $\alpha \approx -2$ at the faint end of the mass function (*e.g.*, Evrard 1989; White & Frenk 1991; Kauffmann, White, & Guiderdoni 1993). However, in practice, observed galaxy samples over large samples usually yield $\alpha \approx -1$ (*e.g.*, Loveday et al. 1995, APM-Stromlo, b_J -band). Steeper faint-end slopes have been found (*e.g.*, Trentham & Tully 2002;

de Propris et al. 2003; Trentham, Sampson, & Banerji 2005), and there is some indication that this is dependent on environment, and on the photometric filter used (*e.g.*, Blanton et al. 2005). Ways of reconciling LFs of the luminous component with the predicted mass function of dark haloes have variously invoked effects of the physics of cooling and ionization (*e.g.*, Chiu, Gnedin, & Ostriker 2001; Somerville 2002).

Recently, with the help of deep photometry of the nearby Universe, the faint end of the LF has been explored in various surveys, revealing features that makes it difficult to fit a single Schechter function to the entire data (*e.g.*, Trentham, Tully, & Mahdavi 2006; Blanton et al. 2005). Indeed, many recent studies suggest that the LF of brighter galaxies ($M_B < -18.5$) should be modelled as a Gaussian, while that of the fainter ones be represented as a Schechter function (*e.g.*, Jerjen 1997; Mahdavi et al. 2005). This approach seeks to explain the peaks and dips in the LF as due to a varying mix of galaxies of different morphological types in different environments, and highlights the connection between the evolution of galaxies and their local environment.

A good example is the luminosity function of galaxies in Hickson compact groups, where a prominent deficit (“dip”) was found at intermediate luminosities (Hunsberger et al. 1998), showing that a single Schechter function would be inadequate to de-

* E-mail: tm@star.sr.bham.ac.uk

scribe these LFs. Indeed, even in the Coma cluster, various studies (*e.g.*, Thompson & Gregory 1993; Lobo et al. 1997; Tully 2005) have found that optical LF of galaxies in the cluster have features not described by a Schechter function.

In a previous paper (Miles et al. 2004), we presented optical (*B* and *R*-band) LFs of a sample of 25 nearby groups of galaxies, as part of the Group Evolution Multiwavelength Study (Forbes et al. 2006; Osmond & Ponman 2004; Khosroshahi et al. 2004; Raychaudhury & Miles 2006, GEMS), for which we have X-ray luminosities (some have upper limits) from ROSAT PSPC observations. To investigate the overall shape of the LF, we stacked together the LFs of several groups, with galaxies chosen from within $0.3 R_{500}$ from the centre of each group. We found that the LF of the X-ray dim groups ($L_X < 10^{41.7}$ erg s $^{-1}$) were significantly different from those of the X-ray brighter groups, showing a prominent dip, similar to Coma, at around $M_B = -18$. We interpreted this deficiency of intermediate-luminosity galaxies as evidence of rapid evolution through merging, since X-ray dim groups have lower velocity dispersion, which would encourage tidal interaction and merging by means of enhanced dynamical friction.

There have been alternative explanations suggested for the various features seen in LFs. Some have argued (*e.g.*, Ferguson & Sandage 1991; Jerjen 1997) that the total luminosity function of a group or cluster has features due to a varying morphological mix across various systems. Others (*e.g.*, Biviano et al. 1995) have suggested that the apparent dip in the optical LF might actually be an enhancement of the bright end of the LF, due to excess star formation caused by tidal effects in the inner regions of the cluster or group.

We address these issues in this paper. To investigate whether the shape of the optical LF is affected by variation in the star formation properties of galaxies, we examine the near-infrared LFs of a large well-defined sample of groups of galaxies, namely the 60 groups of the GEMS study. The JHK photometry from the 2MASS survey is likely to trace evolved stellar populations and hence the total stellar content of galaxies, and thus can be better compared with galaxy formation models. It also allows us to avoid the effects of extinction that plague optical studies.

In the following section, we analyse 2MASS photometry of galaxies belonging to the 60 GEMS groups, and, by splitting them into two categories based on their X-ray luminosity, compare their *K*-band LFs with our earlier *B*-band LFs for a subset of 25 groups (Miles et al. 2004). In §3, we examine how the luminosity functions of X-ray bright and dim groups change with projected radial distance from group centre. We address the issue of the shape of the LF depending on the mix of various morphological types in §4, where we compute model luminosity functions resulting from the summation of the LFs of individual galaxy types. In the final section, we discuss the implications in the context of the evolution of galaxies in groups. We have used $H_0 = 70$ km s $^{-1}$ Mpc $^{-1}$; $\Omega_0 \equiv \Omega_M = 1$ throughout.

2 NEAR-INFRARED LUMINOSITY FUNCTIONS OF GROUPS

Our sample of 60 nearby groups of galaxies, known as the Group Evolution Multi-wavelength Study (GEMS), is described in detail in Osmond & Ponman (2004) and Forbes et al. (2006). It was compiled to represent a wide variety of groups over a large range stages of evolution. First, a master sample of over 4000 optically identified groups was constructed from the literature, from which

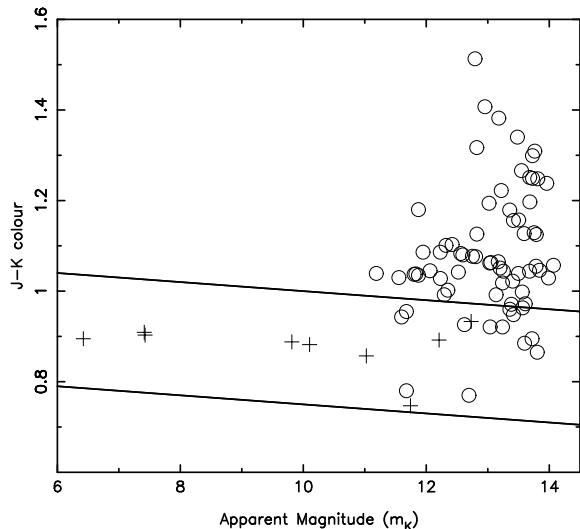


Figure 1. An illustration of the colour-magnitude selection, showing the NGC 4636 group, which has the highest number of known galaxy redshifts in the GEMS sample. Group members, ascertained on the basis of measured redshift, are plotted as crosses, and non-group galaxies as circles. The range of the expected red sequence, as described in the text, is plotted as a pair of lines. The non-group galaxies, within the width of the red sequence down to our magnitude limit ($K = 13.5$), will be removed by our background subtraction method shown Fig. 2

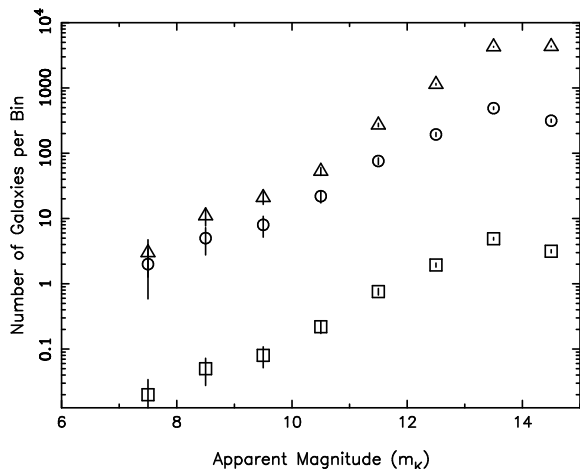


Figure 2. Estimating the background: for each group, we select 100 random fields (of the same area as a R_{500} circle for that group) around it, and compute the total number of galaxies in each *K*-band apparent magnitude bin. Here, triangles represent such a plot for the NGC 5044 group. The circles represent those galaxies that survive the colour-magnitude selection criterion applied from that group. Finally, the squares represent the circles divided by one hundred, this being the “background” histogram to be subtracted when constructing the LF for this group. The trail-off at the faint end shows the incompleteness of the 2MASS catalogue fainter than $M_K=13.75$ (Jarrett 2000).

only those that were found to be within the field of a ROSAT PSPC pointed observation with integration time >10 ks, were chosen as members of the GEMS sample. A large fraction of the GEMS groups were found to have been detected in these pointed PSPC observations, and for the remaining few we have upper limits for their X-ray flux.

2.1 Galaxy Selection and background subtraction

The 2MASS All-Sky Data Release catalogue contains more than 1.6 million extended sources, with a limiting magnitude of $M_K=13.75$ (Jarrett 2000). For each GEMS group, we selected all objects, belonging to the 2MASS All-Sky Extended Source Catalog (2MASX), within a circle of radius R_{500} (radius out to which the mass overdensity is 500 times the mean density of the Universe) of its centre. The adopted group centres, values of R_{500} and distances to these groups can be found in Osmond & Ponman (2004).

The $J - K$ colours were calculated from the isophotal magnitudes ($K_s=20$ mag arcsec $^{-2}$). Galaxies were selected as being likely group members from the red sequences of the colour-magnitude diagram, involving the $(J - K)$ colour and the K_s magnitude. The width of the red sequence was based on the Coma Cluster $U - V$ colour-magnitude relation of Terlevich, Caldwell & Bower (2001), its 3σ width being converted to a $J - K$ width based on Jarrett (2000).

Fig. 1 illustrates this for the case of the NGC 4636 group, which has the highest number of known galaxy redshifts in the GEMS sample. It has 80 measured redshifts within R_{500} (most GEMS groups have under 10 measured redshifts within this radius and 21 groups have under 5 redshifts). The colour-magnitude diagram shows group galaxies as crosses, and non-group galaxies as circles. The non-group galaxies that are within the $3 - \sigma$ are all faint and are then removed by our background subtraction method. out to the magnitude limit used here ($K < 13.5$).

Given that the number of galaxies in each group is small, the luminosity functions may be affected significantly by the method of background subtraction. For this reason, for each group, we took a large sample of field galaxies from 100 randomly-selected, independent, regions on the sky, each of radius equal to the value of R_{500} for the group. We then calculated the mean number of galaxies occupying each magnitude bin and subtracted them from the target group. The whole process was then repeated for every group in the GEMS sample.

Fig. 2 shows one such example, where the raw number of galaxies found in these field regions is shown as triangles, binned in apparent K_s magnitude. Open circles show all field galaxies from these 100 regions satisfying the C-M selection criterion for the group. The open squares show those galaxies surviving the C-M cut divided by 100, representing the average number of local background and foreground galaxies expected in each bin of apparent magnitude. In this way we aimed to account for cosmic variance and to have compiled as unbiased a selection of field galaxies as possible.

3 LUMINOSITY FUNCTIONS OF X-RAY BRIGHT AND DIM GROUPS

Since the number of member galaxies in each individual group is small, the galaxian luminosity function (LF) of the groups was evaluated by co-adding galaxies of several groups in equally spaced bins of absolute luminosity.

An apparent magnitude cut-off was adopted at $K = 13.5$, since Fig. 2 shows that the samples of 2MASS galaxies, in 100 randomly-selected field regions, is reasonably complete to $K \sim 13.75$ (cf. Jarrett 2000). The resulting limit in absolute magnitude varies between groups— the distance moduli of the 60 groups range between 30.1 and 35.5, with the median of 32.5. Hence, co-added LFs were evaluated by dividing the number of co-added galaxies in each bin

of absolute magnitude by the number of contributory groups to that bin. When plotting the group LFs, we chose a conservative absolute magnitude limit of $M_K < -20$ so that the faintest bin contains over half of groups within the 2MASS completeness limit of $K < 13.5$.

Various optical and X-ray properties of GEMS groups may be found in Osmond & Ponman (2004) and Forbes *et al.* (2006). The groups in our sample represent very diverse systems in terms of their content and physical properties. We divide our sample of galaxies into two sub-classes according to the X-ray luminosity of their parent groups, which is related to the mass and velocity dispersion of the latter.

As in Miles *et al.* (2004), we use the X-ray luminosities measured by Osmond & Ponman (2004), who used ROSAT PSPC observations in the 0.5–2 keV range, fitting β -profiles after point source removal, extrapolated to estimate the bolometric X-ray luminosity. We characterised the parent groups as X-ray bright if their bolometric X-ray luminosity is more than the median of the sample, $L_X = 10^{41.7}$ erg s $^{-1}$, and X-ray dim if less. This X-ray luminosity refers to that of the group plus of any central galaxy that might exist.

3.1 Stacked Near-Infrared Luminosity Functions within $0.3R_{500}$

The differential galaxian Luminosity Functions of the 25 GEMS Groups that made up our earlier optical sample (Miles *et al.* 2004) above are shown in Fig. 3 in B and K -bands, out to $0.3R_{500}$, for direct comparison between the optical and near-IR LFs. As in the optical LFs (B , as shown here, and in R) analysed in Miles *et al.* (2004), a clear difference between the LFs of the X-ray bright groups and X-ray dim groups is evident, with a depletion in the number of galaxies with magnitudes between $-24 < M_K < -23$ and $-23 < M_J < -22$ for the latter category of groups. The possibility that these dips are due to some of the galaxies being systematically missed can be ruled out. As is apparent from Fig. 2, our 2MASS sample is complete to about four magnitudes fainter than the position of the dip in the luminosity function.

The previous pair of figures represented the combined LFs in the two categories out to $0.3R_{500}$ from the centres of only the 25 groups covered in the Miles *et al.* (2004) study, so that the K -band LF could be directly compared with the optical results. In the optical study, however, the number of groups studied and the area of sky covered in the case of each group were limited by the availability of observing time, and the size of the wide-field CCD arrays we had been using.

In this paper, our near-IR magnitudes come from the 2MASS survey, so we can deal with the whole GEMS sample of 60 groups, as well as go out in radius further than the previous study. We do the latter in the next section, but here in Fig. 4 we plot the J and K -band differential Luminosity Functions of the entire GEMS sample- all 60 Groups of galaxies, including those plotted in Fig. 3, each within a radius of $0.3R_{500}$ from their respective centres, stacked together to form a composite LF for the respective sub-classes. There are 39 X-ray dim and 21 X-ray bright groups in this sample, and the total number of galaxies in either category is similar.

As in Fig. 3, it is clear that the LFs of the dim groups show “dips” in the LFs between $-23 < M_J < -22$ and $-24 < M_K < -23$, thus showing that the GEMS sub-sample chosen in the Miles *et al.* (2004) work was representative, and that the near-IR LFs are similar, irrespective of the filter used.

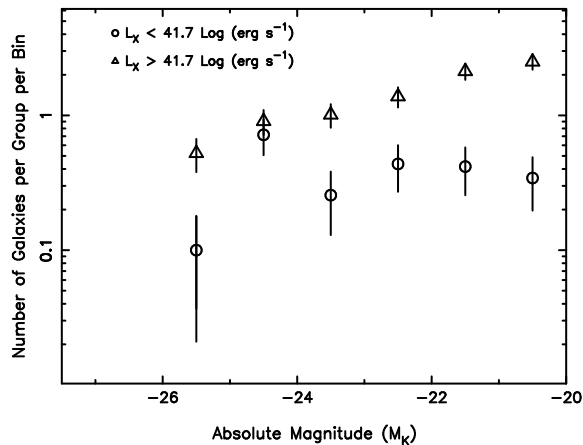


Figure 5. The K -band differential Luminosity Function of the GEMS sample, without the brightest galaxy in each group, plotted on the same scale as Fig. 4b to allow direct comparison. The brightest two bins are diminished, whilst the dipping feature found in Fig. 4 remains.

One possible reason for finding a dip feature fainter than the bright end of the LF of groups is that it could result from the fact that in most poor groups, there is one dominant galaxy, which would account for an enhancement of galaxies towards the bright end of the LF. We examine whether this is the case of the GEMS LFs, by plotting in Fig. 5, the K -band differential Luminosity Function of all 60 groups (same as in Fig. 4b), but without the brightest group galaxies, plotted on the same scale as Fig. 4b) to allow direct comparison. As expected, no galaxies remain in the brightest bin, and there are fewer in the second brightest, but the dip feature remains, showing that the brightest group galaxies do not account for the appearance of this feature. The LFs without the central brightest galaxy are similar in the other optical and near-IR filters.

3.2 Luminosity Functions as a Function of Radius

Differential K -band Luminosity Functions of all X-ray dim and X-ray bright GEMS groups are shown in Fig. 6. The groups in each category are stacked together in radial bins upto $0.3 R_{500}$, upto $0.6 R_{500}$ and upto $1.0 R_{500}$. It is clear that the LF of the X-ray dim groups show a deficiency in the LF between $-24 < M_K < -23$ within $0.3 R_{500}$, together with a flattening in the fainter galaxies at magnitudes $M_K > -22$.

Fig. 7 shows in detail how dividing the sample into radial annuli, rather than the integrated average out to a certain radius as shown in Fig. 6, illustrates explicitly the difference in LF shape in the central regions of X-ray dim groups. The dip between $-24 < M_K < -23$ seen in the LF in the central regions of the groups gradually disappears as the LF is averaged out to larger radii, approaching R_{500} .

Furthermore, when averaged out to large distances ($\sim R_{500}$) from the centres of the groups, X-ray bright and X-ray dim groups have similar LF shapes (see Fig. 6). Taking all galaxies out to R_{500} , the K-S test shows that it is not possible to distinguish between the two samples at the 92% confidence level.

3.3 The slope at the faint end of the LF

Another feature of the LF to note in Figs. 3 and 4 is the relative flattening of the LF in the K -band at the faint end compared to the B -band, particularly in the cores of the X-ray dim groups

($< 0.3 R_{500}$). One possibility is that it could result from enhanced recent star formation activity being revealed in the B -band and not in the JHK bands. Tidal interactions in the densest regions of these dynamically young groups may be responsible for preferentially inducing star formation in the less massive galaxies.

Another reason for the difference in faint end slope between B and K band data for X-ray dim groups could be the bias against low surface brightness galaxies in the 2MASS catalogue, as discussed by the original study of galaxies in the survey (Bell et al. 2003). We test this by examining the morphology of all member galaxies in the B image individually by eye, and classifying them as early or late-type. Fig 8 shows the ratio of early to late type galaxies in absolute B magnitude bins, for the X-ray bright groups (solid line) and X-ray dim groups (dotted line).

This shows that at the faint end, the fraction of early-type galaxies, as identified from optical images, is significantly higher in the X-ray bright groups. The faint end of the LF of X-ray faint groups has a higher dominance of late-type galaxies than in X-ray bright groups. If low surface brightness late-type galaxies are systematically missed in the 2MASS survey, this would account for the flattening of the LF at the faint end, compared to that in the B -band,

4 THE MORPHOLOGICAL CONTENT OF GROUPS

It is important to compare our results with previous studies utilising the 2MASS catalogue. Balogh et al. (2001) use the second incremental release data from 2MASS to build a composite LF for clusters, based on 274 cluster galaxies with redshift measurements from the Las Campanas Redshift Survey. Despite the large scatter due to the small number of galaxies in their sample, they find best fit values for the Schechter parameters $M_{K^*} = -23.8 \pm 0.4$ and $\alpha = -1.30 \pm 0.43$ in clusters, $M_{K^*} = -23.5 \pm 0.1$ and $\alpha = -1.14 \pm 0.26$ in groups and $M_{K^*} = -23.4 \pm 0.1$ and $\alpha = -1.12 \pm 0.21$ in the field. On the other hand, Y-T Lin et al. (2004) use the full 2MASS data release to produce K -band LFs of galaxies within 93 galaxy clusters and groups, including the three GEMS groups, NGC 2563, NGC 6338 and HCG 62. They found difficulties fitting a single Schechter function to their data and resorted to the removal of the brightest galaxies from their fitting procedure to produce $M_{K^*} = -24.02 \pm 0.02$ and $\alpha = -0.84 \pm 0.02$. i.e., they obtained a higher M_{K^*} than Balogh et al. (2001) and a flatter α parameter.

4.1 LFs of various morphological types

Solutions to the problem of the inadequacy of a single Schechter function fit have been found when meeting dipping features in the LF of a number of structures ranging in mass from the Coma (Andreon & Pelló 2000), Virgo and Fornax clusters (Ferguson & Sandage 1991) to Hickson groups (Hunsberger et al. 1998) and the Leo I group (Flint, Bolte, & Mendes de Oliveira 2003).

Attempts have been made to explain these features as the consequence of the observed LF being just the superposition of a number of underlying LFs, each describing that of a different morphological type of galaxies, and the variation in the LF would then just be due to the variation in the relative abundances of the different contributing galaxy types.

To test this hypothesis, we perform the following test. We start from the B -band LF of both X-ray bright and X-ray dim groups,

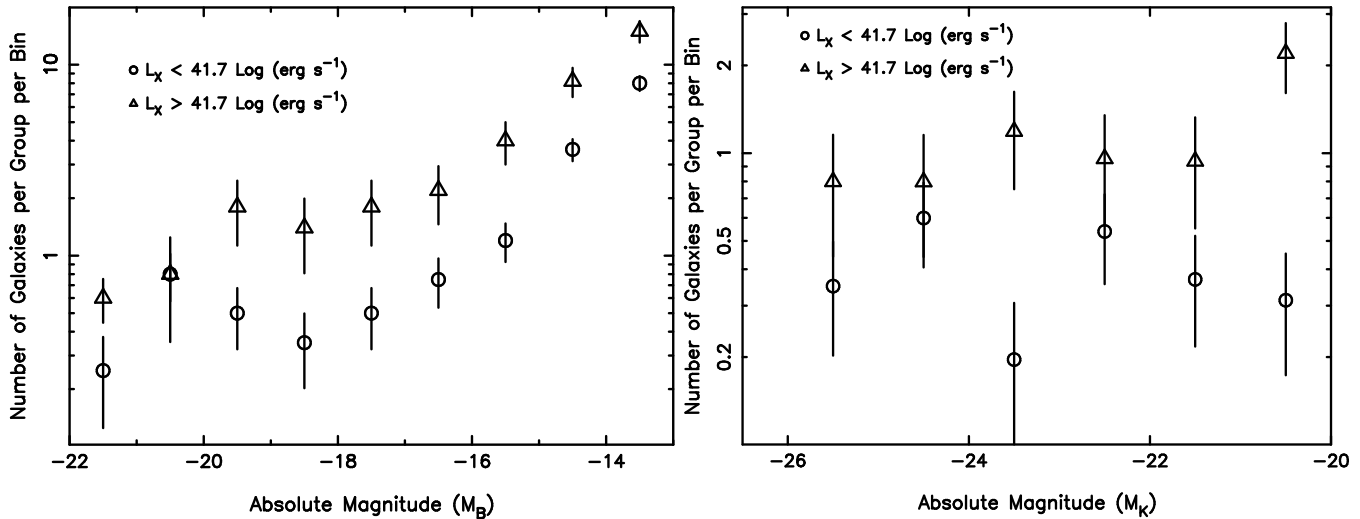


Figure 3. The mean differential Luminosity Functions of 25 GEMS Groups of galaxies, in the B -band (left) and K -band (right), each within a radius of $0.3R_{500}$ from their respective centres, stacked together to form a composite LF for the respective sub-classes. These groups are the same as those described in Miles *et al.* (2004). Here X-ray bright groups ($L_X > 10^{41.7}$ erg s^{-1} , triangles) and X-ray dim groups ($L_X < 10^{41.7}$ erg s^{-1} , circles). It is clear that the LFs of the dim groups show “dips” in the LFs between $-19 < M_B < -17$ and $-24 < M_K < -23$.

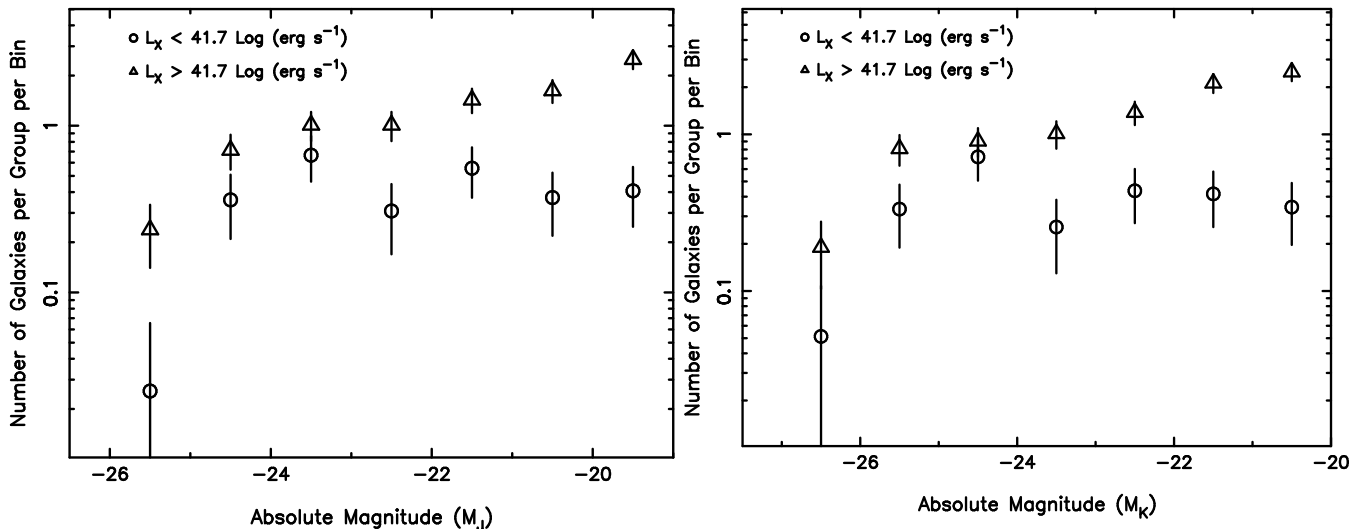


Figure 4. The near-infrared mean differential Luminosity Functions of the entire GEMS sample- all 60 Groups of galaxies, in the J -band (left) and K -band (right), each within a radius of $0.3R_{500}$ from their respective centres, stacked together to form a composite LF for the respective sub-classes. As in Fig. 3, X-ray bright groups ($L_X > 10^{41.7}$ erg s^{-1}) are plotted as triangles, and X-ray dim groups ($L_X < 10^{41.7}$ erg s^{-1}) as circles. It is clear that the LFs of the dim groups show “dips” in the LFs between $-23 < M_J < -22$ and $-24 < M_K < -23$.

within a radius of $0.3R_{500}$, as obtained in Miles *et al.* (2004). We treat them as a superposition of five different kinds of LFs, each for a different morphological type (Ellipticals, S0s, Spirals, Dwarf Irregulars and Dwarf Ellipticals). We then correct each component LF for the $B - K$ colour appropriate for that morphological type and ask whether the resultant K -band LF resembles the observed one. If the variation of the observed LFs are solely due to a varying fraction of the different morphological types, the predicted LFs found this way should match the observed ones.

The type-specific LFs are not necessarily of the Schechter form but may take Gaussian shapes (Jerjen 1997, 2001). In the case of elliptical, S0 and spiral galaxies, we use Gaussian LFs, and for the dwarf early and late types we use Schechter functions, following the Jerjen (2001) prescription (see Table 1).

Table 1. Analytical functions and fixed parameters for the adopted type-specific Luminosity Functions (following Jerjen 2001).

Galaxy Type	Function	Parameter 1	Parameter 2
Elliptical	Gaussian	$\overline{M_B} = -18.3$	$\sigma_{(M < \overline{M_B})} = 2.2$ $\sigma_{(M > \overline{M_B})} = 1.3$
S0	Gaussian	$\overline{M_B} = -18.9$	$\sigma = 1.1$
Spiral	Gaussian	$\overline{M_B} = -18.3$	$\sigma = 1.4$
dIrr	Schechter	$M_B^* = -16.2$	$\alpha = -1.0$
dE	Schechter	$M_B^* = -17.8$	$\alpha = -1.4$

Markov chain Monte Carlo (MCMC) fitting was used to determine the best-fit total B -band composite LF from the five compo-

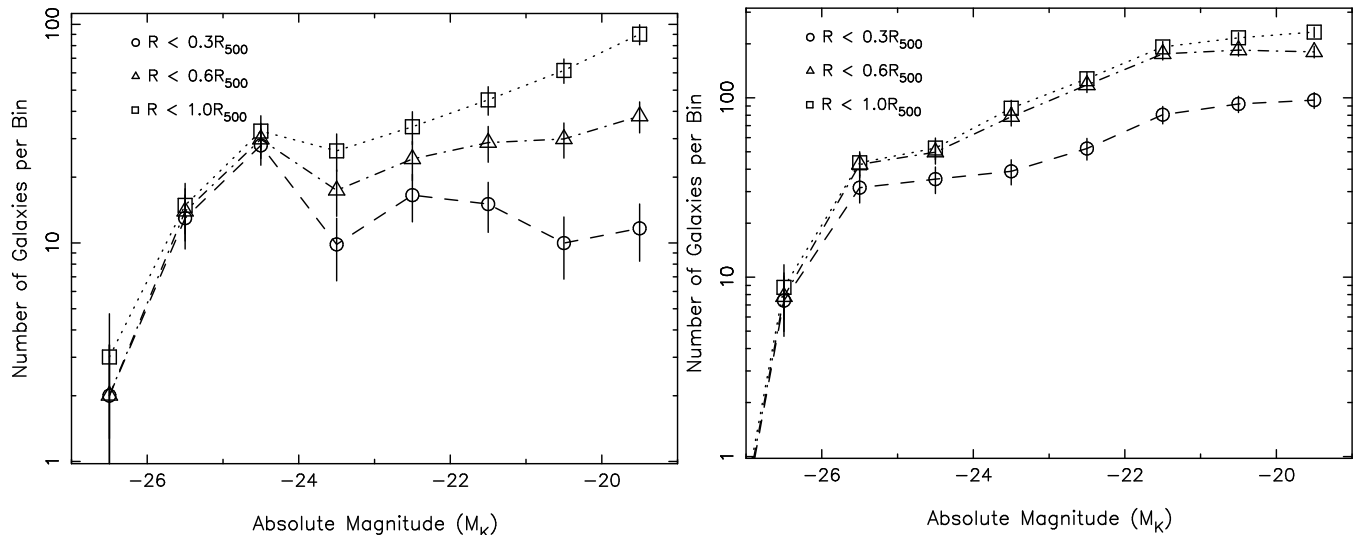


Figure 6. K -band composite differential luminosity function of (Left): all 39 X-ray dim groups ($L_X < 10^{41.7}$ erg s $^{-1}$), interior to a fraction of the projected group radius, and (Right): all 21 high X-ray luminosity groups ($L_X > 10^{41.7}$ erg s $^{-1}$). The three plots in each case go out to 0.3, 0.6 and 1.0 times R_{500} respectively. The intermediate luminosity dip feature is more prominent in the inner regions of the X-ray dim groups. The LF of the X-ray bright groups remains similar in shape at all radii.

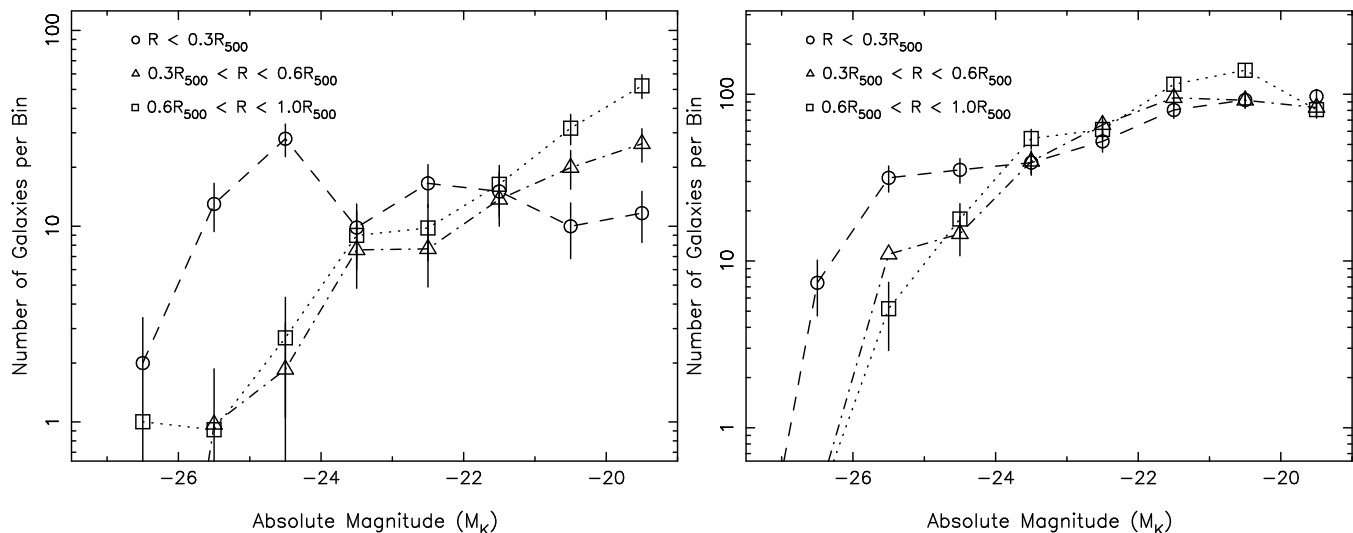


Figure 7. As in the previous figure, but in differential radial bins. (Left): The K -band luminosity function of all X-ray dim groups ($L_X < 10^{41.7}$ erg s $^{-1}$) and (Right): all X-ray bright groups ($L_X > 10^{41.7}$ erg s $^{-1}$), divided into annuli of projected radius. The inner $0.3R_{500}$ of the X-ray dim groups shows a luminosity function of a significantly different shape, in comparison with both the high X-ray luminosity groups at all radii and also with the outer regions of the X-ray dim groups themselves.

nent LFs, for both the X-ray faint (Fig. 9a) and X-ray bright groups (Fig. 10b). The MCMC algorithm (e.g., Lewis & Bridle 2002) is a computationally efficient way to map the likelihood of the fit to the data in the high-dimensional parameter space of the five LF components. The MCMC algorithm was used to draw samples with a number density asymptotically proportional to the probability density representing the likelihood of the fit. In this way, the shape of the full posterior probability density (using a uniform prior) was explored while avoiding excessive processor time in low-probability regions of the fit-space.

The MCMC algorithm selected new points in the fit-space by simultaneously jumping along all the parameters representing the five LF components. The size of this jump was always a random fraction of a characteristic step-size along each parameter. The chi-

Table 2. $B-K$ colours for galaxies used to convert B -band LFs to K -band LFs in Figs. 9 and 10 (after Jarrett 2003).

Galaxy Type	$B_{\text{Total}}-K_{\text{Total}}$
Elliptical	4.0
S0	4.1
Spiral	3.2
dIrr	4.1
dE	4.0

squared statistic at this new point was then evaluated, and the new point accepted or rejected. The process was then repeated, jumping again from the most recently accepted point in the fit-space. The

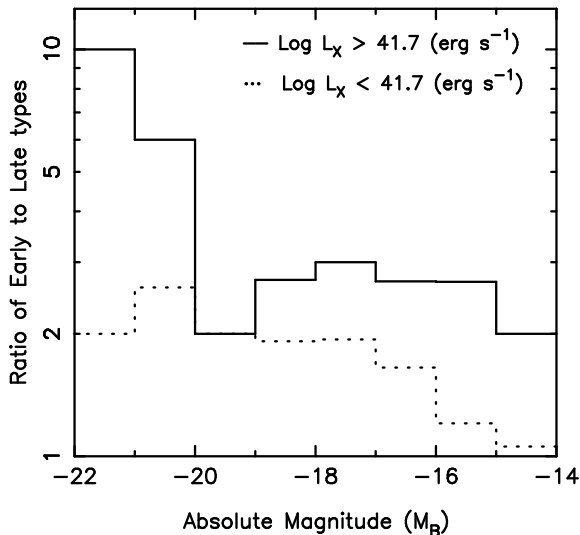


Figure 8. The ratio of early to late type galaxies (where morphology is assigned by visual inspection from optical CCD images), divided into X-ray bright ($L_X > 10^{41.7} \text{ erg s}^{-1}$) and X-ray dim ($L_X < 10^{41.7} \text{ erg s}^{-1}$) groups. The relative abundance dominance of late-type dwarf galaxies in the X-ray dim groups may account for the flattening of the faint end of their near-IR luminosity function, if low surface brightness objects are being systematically missed in the 2MASS survey.

number of accepted points was optimised by adjusting the step-size along each component. Excessively large step sizes meant that very few new points were accepted, and overly small step sizes restricted exploration around the fit-space. The algorithm had clearly determined a best-fit curve from the five components after 10^7 iterations.

Fig. 9a shows the results of the fitting procedure, plotted superposed on the observed B -band data, for the X-ray dim groups. The best-fit component LFs were corrected by the colour appropriate for the particular morphological type using the typical $B-K$ colours for each morphological type, as given in Jarrett et al. (2003) and shown in Table 2, and the predicted composite K -band luminosity function is shown in Fig. 9b. Superposed on these are the observed LFs.

It is obvious that this procedure would not work if it is required to fit both the B and K band LFs simultaneously. The K -band LFs produced from the B -band observed data do not have the same features as the observed K -band LFs. In order to find a good match to the observed K -band LFs, one expects the B -band LF to be dominated almost exclusively by ellipticals and S0s brighter than -18 , and the number of spirals to be insignificant.

For the X-ray bright groups, shown in Fig. 10, early types dominate the brighter end, and again there are very few spirals brighter than -18 , contrary to what is observed.

4.2 Comparison with visually verified morphological content

We can go one step further and check the morphological composition of these groups from our visual inspection of galaxy images in the X-ray dim groups.

The visual classification used here is the same as that used in Miles et al. (2004), further details may be found therein. A simple classification system was adopted whereby each galaxy was classified as early- or late-type based on inspecting the B -band optical CCD image. The relative content of early and late type galaxies,

thus determined, is shown in Fig. 11, and compared with the relative abundances predicted by the LF fits in the previous section.

The component LF-fitting process predicts the presence of large numbers of dwarf irregulars in the B -band (Fig. 9, dotted line), which seems to be a reasonable fit to the data (Fig. 9b (dotted line); Fig. 11b, dotted line). However, the model fails to fit the dwarf elliptical population (dot-dot-dot-dashed line), underestimating the observed frequency in Fig. 11a. The spiral galaxy population is missed entirely by the models (Fig. 11b, dash-dot-dot-dot line). The predicted early-type population (elliptical and lenticulars) matches the observed data better than the late-type curve but also fails to pass through any data point within error bars.

The apparent failure of the component morphology-based LF curves to fit real data indicates that the galaxy population in groups of galaxies has a different morphological mix from that of clusters and in the field. Evolutionary processes are most favoured in groups and may be responsible for the differences in galaxy populations observed.

5 DISCUSSION AND CONCLUSIONS

The main problems associated with Luminosity Functions at optical wavelengths are that they are liable to be affected by dust extinction as well as by young stellar populations, thus rendering the light less representative of the underlying matter. This is far less of a problem in the near-infrared, where one is more likely to trace the more evolved stellar populations and hence the actual stellar content of galaxies. Near-infrared luminosities are more directly related to stellar mass, constraining both the history of the star formation and galaxy formation models. The fact that we find dip features in the luminosity functions of X-ray dim groups of galaxies in the near-infrared regime means that it is unlikely that star formation or dust extinction is responsible for the observed depletion of intermediate magnitude galaxies.

Such features have often been explained as the result of the representation in the total galaxy luminosity function of the underlying morphological makeup of groups. Invariant type-specific LFs have been claimed (*e.g.*, Jerjen 2001). Implicit in this notion is the assumption of passive evolution at all structure scales, and thus the shape of the LF is merely due to the combination of the individual LFs of galaxies of different morphological types in varying proportions. The deviation from these functional forms may therefore provide evidence of predominant major mergers affecting this model, and bringing into question the invariance of the LFs of individual morphological types.

Fig. 11 shows the observed luminosity function of galaxies visually classified as early and late types. The superposed curves are the results from the earlier fitting process, clearly showing that the comparison with real data does not work when one assumes universal luminosity functions for different morphological types. This view subscribes to the notion of passive evolution *i.e.*, an initial distribution of galaxy types was imprinted in the early Universe and very little has occurred by way of galaxy transformational processes (such as major or minor galaxy mergers, ram pressure stripping, and harassment) to affect this makeup. This view falters when confronted with the high incidence of early-type galaxies in the relatively shallow potential wells of groups.

We argued in Miles et al. (2004) that the persistent depletion of the intermediate-luminosity galaxies in the optical luminosity functions of X-ray dim groups shows that in the dynamically sluggish environment of such groups (which have low velocity disper-

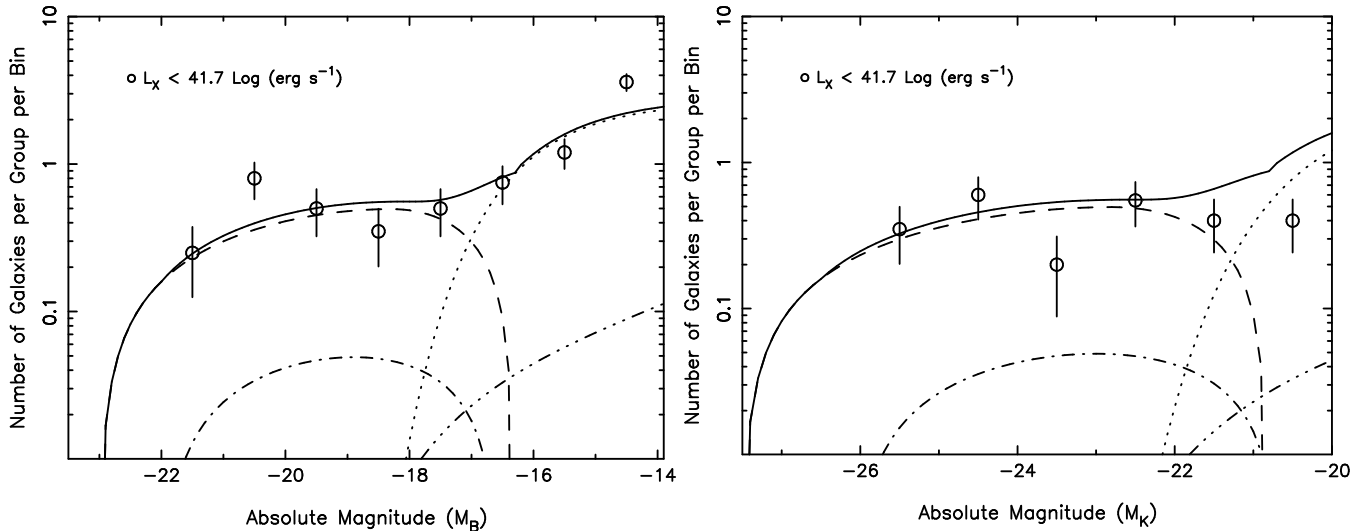


Figure 9. [Left] The best fit five-component LFs, one for each morphological type (Ellipticals, S0s, Spirals, Dwarf Irregulars and Dwarf Ellipticals), following the Jerjen (2001) functional forms (see Table 1), that add up to form the best model B -band LF. Also plotted are the observed data, averaged for 20 X-ray dim groups ($L_X < 10^{41.7} \text{ erg s}^{-1}$) out to $0.3R_{500}$. Here the dashed line = Ellipticals; dash-dot = S0s; dot-dot-dot-dash = dEs; dotted line = dIrrs & continuous line = sum of all components). According to these fits, spirals make a negligible contribution to the morphological makeup, contrary to observations [Right] The predicted K -band LFs of the five components, using the same line styles, together with the observed LF from the 2MASS analysis in this paper.

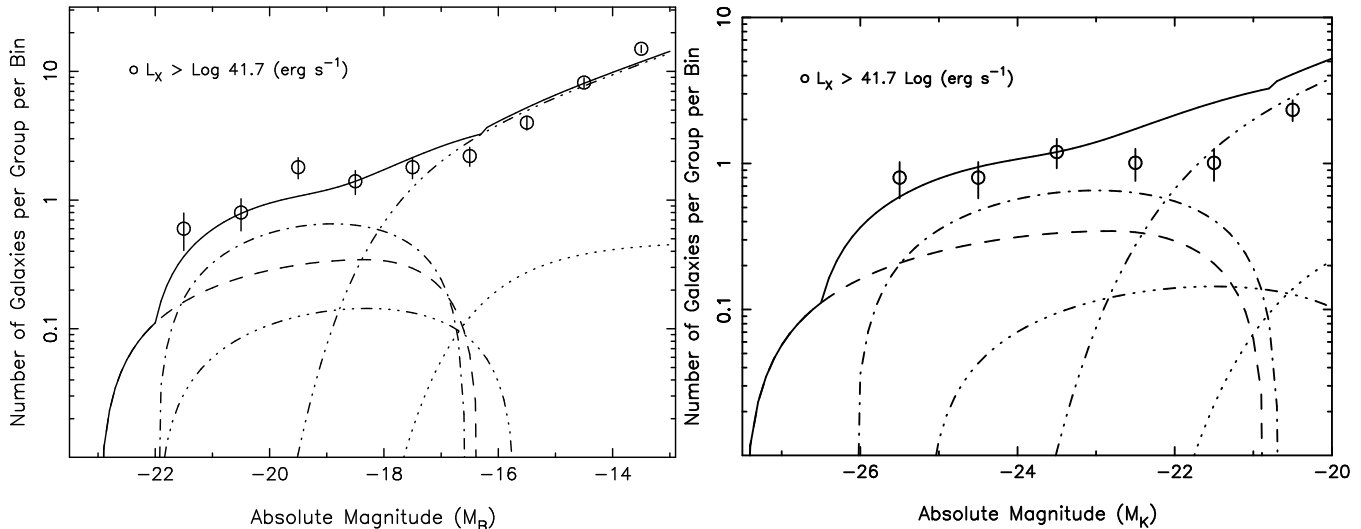


Figure 10. [Left] B -band LFs, similar to Fig. 9, but for the X-ray bright groups ($L_X > 10^{41.7} \text{ erg s}^{-1}$), in our optical sample, out to $0.3R_{500}$. [Right] Corresponding predicted K -band LFs of the individual components, together with the observed LF from the 2MASS analysis in this paper. The line style used for the various types is the same as before. In this case, Spirals (= dash-dot-dot-dot, centred on $M_B = -18.3$) feature in the fitting process.

son), dynamical friction would facilitate more rapid merging, thus depleting intermediate-luminosity galaxies to form a few giant central galaxies, resulting in the prominent dip seen in our LFs. In this work, we have shown that this effect is also seen in the near-infrared LFs, but only in the interior regions of the groups ($R < 0.3 R_{500}$), as in the case of the optical LFs. We also show that this effect vanishes when one goes out to R_{500} , an effect we had not tested in our optical CCD data due to lack of coverage. We thus show that the intermediate depletion in the LFs is a real feature, and we argue that it is due to the merging of galaxies, rather than a bright-end enhancement caused by excess star formation.

ACKNOWLEDGEMENTS

Thanks to Trevor Ponman for interesting discussions and suggestions, and, together with John Osmond, for their work on the X-ray properties of the GEMS sample, and to Duncan Forbes and all our collaborators in the multi-wavelength GEMS project. This publication makes use of data products from the Two Micron All Sky Survey, which is a joint project of the University of Massachusetts and the Infrared Processing and Analysis Center/California Institute of Technology, funded by the National Aeronautics and Space Administration and the National Science Foundation. This research has also made use of the NASA/IPAC Extragalactic Database (NED) which is operated by the Jet Propulsion Laboratory, California In-

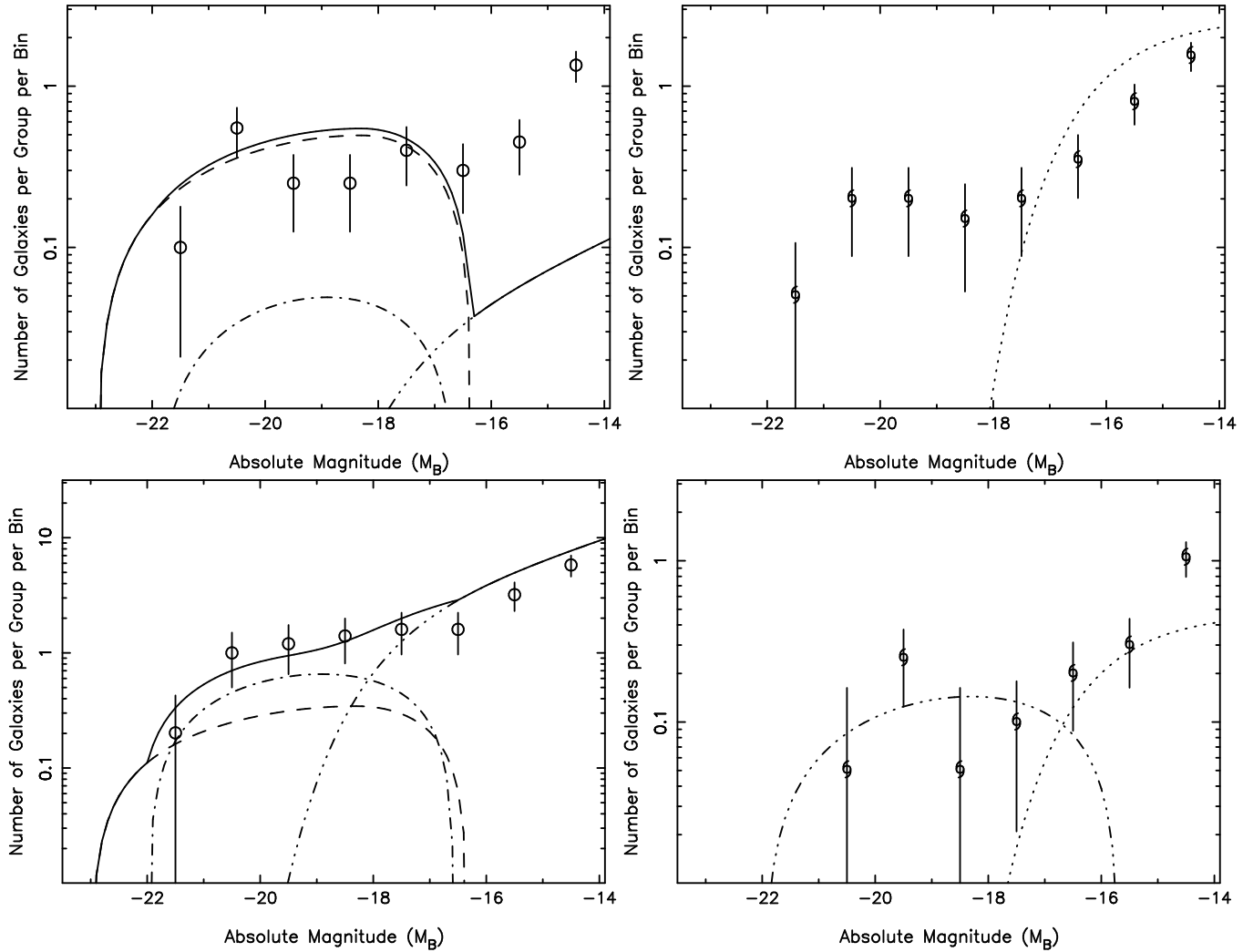


Figure 11. The four panels show observed B -band luminosity functions for the Early-type galaxies (circles) and late-type galaxies (spirals). The top two panels are for X-ray dim groups ($L_X < 10^{41.7} \text{ erg s}^{-1}$), and the two bottom panels for X-ray bright groups ($L_X > 10^{41.7} \text{ erg s}^{-1}$), both out to $0.3R_{500}$. Shown for comparison are the best fit component LFs from Figs. 9 and 10. **[Left]** Ellipticals = dashed line; S0s = dash-dot; dEs = dash-dot-dot-dot; continuous line = sum of all components. **[Right]** Spirals = dash-dot-dot-dot; dIrrs = dotted line.

[Top Left] Data points: Early-type galaxy B -band LF for X-ray dim groups. Curves: Early-type components fitted to total X-ray dim group LF.

[Top Right] Data points: Late-type galaxy B -band LF for X-ray dim groups. Curves: Late-type components fitted to total X-ray dim group LF.

[Bottom Left] Data points: Early-type galaxy B -band LF for X-ray bright groups. Curves: Early-type components fitted to total X-ray bright group LF.

[Bottom Right] Data points: Late-type galaxy B -band LF for X-ray bright groups. Curves: Late-type components fitted to total X-ray bright group LF. This exercise shows that the morphological abundances from the best-fit model LFs do not match the observations.

stitute of Technology, under contract with the National Aeronautics and Space Administration.

REFERENCES

- Andreon, S. & Pello, R., 2000, *A&A*, 353, 479
 Balogh, M. L., Christlein, D., Zabludoff, A. I., & Zaritsky, D. 2001, *ApJ*, 557, 117
 Bell, E. F., McIntosh, D. H., Katz, N. & Weinberg, M. D., 1996, *A&AS*, 117, 393
 Benson A.J., Bower R.G., Frenk C.S., Lacey C.G., Baugh C.M., Cole, S., 2003, *ApJ*, 599, 38B
 Bertin, E. & Arnouts, S., 1996, *A&AS*, 117, 393
 Biviano A., Durret F., Gerbal D., le Fevre O., Lobo C., Mazure A., & Slezak E., 1995, *A&A*, 297, 610
 Blanton, M. R., Lupton, R. H., Schlegel, D. J., Strauss, M. A., Brinkmann, J., Fukugita, M., & Loveday, J., 2005, *ApJ*, 631, 208
 Chiu W. A., Gnedin N. Y., Ostriker J. P., 2001, *ApJ*, 563, 21
 Cole, S., Lacey, C., Baugh, C., & Frenk, C., 2000, *MNRAS*, 319, 168
 de Oliveira, C.M. & Hickson, P., 1991, *ApJ*, 380, 30
 de Propriis R. et al. 2003, *MNRAS*, 342, 725
 Evrard A. E., 1989, *ApJ*, 341, 26
 Ferguson, H.C. & Sandage, A.R., 1991, *AJ*, 101, 765
 Forbes D. A., Ponman, T., Pearce, F., Osmond, J., Kilborn, V., Brough, S., Raychaudhury, S., Mundell, C., Miles, T., Kern, K. 2006, *PASA*, 23, 38
 Flint K., Bolte M. & Mendes de Oliveira C., 2003, *Ap&SS*, 285, 191
 Hunsberger, S., Charlton, J. & Zaritsky, D., 1998, *ApJ*, 462, 50
 Jarrett, T.H., 2000, *PASP*, 112, 1008

- Jarrett, T.H., Chester, T., Cutri, R., Schneider, S.E. & Huchra, J.P., 2003, *AJ*, 125, 525
- Jerjen, H. & Tammann, G. A., 1997, *A&A*, 321, 713
- Jerjen, H., 2001, *Encyclopedia of Astronomy and Astrophysics*, McMillan, Bristol
- Kauffmann G., White S. D. M., Guiderdoni B., 1993, *MNRAS*, 264, 201
- Kauffmann G., Colberg J.M., Diaferio A., White, S.D.M., 1999, *MNRAS*, 303, 188
- Khosroshahi H., Raychaudhury S., Ponman T.J., Miles T. A. & Forbes D. A. 2004. *MNRAS*, 349, 527
- Lewis A., Bridle S., 2002, *PhRvD*, 66, 103511
- Lin, Y-T, Mohr, J.J. & Stanford, S. A., 2004, *ApJ*, 610, 745
- Lobo C., Biviano A., Durret F., Gerbal D., Le Fevre O., Mazure A., & Slezak E., 1997, *A&A*, 317, 385
- Loveday, J., Maddox, S.J., Efstathiou, G., & Peterson, B.A., 1995, *ApJ*, 442, 457
- Mahdavi A., Trentham N. & Tully R. B. 2005, *AJ*, 130, 1502
- Miles T.A., Raychaudhury S., Forbes D.A., Goudfrooij, P., Ponman T.J. & Kozhurina-Platais, V., 2004, *MNRAS*, 355, 785
- Nolan L. A., Dunlop J. S., Jimenez R. & Heavens A. F., 2003, *MNRAS*, 341, 464
- Osmond J. P. F., Ponman T. J., 2004, *MNRAS*, 350, 1511
- Raychaudhury S. and Miles T. A., 2006, proceedings of the ESO workshop "Groups of galaxies in the Nearby Universe", held in Santiago, December 2005, ed. I. Saviane, V. Saviane & J. Borissova
- Somerville R. S., 2002, *ApJ*, 572, L23
- Somerville, R.S., Primack, J.R., 1999, *MNRAS*, 310, 1087
- Terlevich, A.I. & Forbes, D.A., 2002, *MNRAS*, 330, 547
- Terlevich, A.I., Caldwell, N. & Bower, R. G., 2001 *MNRAS* 326, 1547
- Thompson, L.A., Gregory, S.A. 1993, *AJ*, 106, 2197
- Trentham N., Tully R. B., Mahdavi A., 2006, *MNRAS*, 369, 1375
- Trentham N., Sampson L., Banerji M., 2005, *MNRAS*, 357, 783
- Trentham N., Tully R. B., 2002, *MNRAS*, 335, 712
- Tully R. B. 2005, Proceedings of IAUC 198 "Near-Field Cosmology with Dwarf Elliptical Galaxies" (astro-ph/0505047).
- Turner, E. L., Gott, J.R., 1976, *ApJ*, 209, 6T
- White, S.D.M., Rees, M.J. 1978, *MNRAS*, 183, 341
- White S. D. M., Frenk C. S., 1991, *ApJ*, 379, 52
- Zabludoff, A.I. & Mulchaey, J.S., 2000, *ApJ*, 539, 136
- Zepf, S. E., Whitmore, B. C., 1991, *ApJ*, 383, 542